JVSTA Journal of Vacuum Science & Technology A

Dissociation of trimethylgallium on the ZrB2(0001) surface

Kedar Manandhar, Michael Trenary, Shigeki Otani, and Peter Zapol

Citation: Journal of Vacuum Science & Technology A **31**, 061405 (2013); doi: 10.1116/1.4826881
View online: http://dx.doi.org/10.1116/1.4826881
View Table of Contents: http://scitation.aip.org/content/avs/journal/jvsta/31/6?ver=pdfcov
Published by the AVS: Science & Technology of Materials, Interfaces, and Processing

Dissociation of trimethylgallium on the $ZrB_2(0001)$ surface

Kedar Manandhar and Michael Trenary[a)]
Department of Chemistry, University of Illinois at Chicago, 845W Taylor St., Chicago, Illinois 60607

Shigeki Otani
National Institute for Material Science, 1-1 Namiki, Tsukuba-shi, Ibaraki 305-0044, Japan

Peter Zapol
Materials Science Division, Argonne National Laboratory, 9700 S. Cass Ave., Argonne, Illinois 60439

(Received 1 August 2013; accepted 11 October 2013; published 29 October 2013)

X-ray photoelectron spectroscopy and reflection absorption infrared spectroscopy (RAIRS) have been used to study the dissociative adsorption of trimethylgallium (TMG) on the $ZrB_2(0001)$ surface. Spectra were obtained as a function of annealing temperature following TMG exposure at temperatures of 95 and 300 K, and also as a function of TMG exposure for a surface temperature of 300 K. After annealing above 220 K, a significant decrease in the relative concentration of carbon and gallium occurred accompanied by a shift of ~0.2 eV in the Ga $2p_{3/2}$ binding energy. The RAIR spectra show that after annealing to ~220 K, only one CH_3 deformation band at 1196 cm^{-1} remains, the intensity of which is considerably decreased indicating loss of at least one methyl group from TMG. Further annealing leads to the sequential loss of the other methyl groups. The first methyl desorbs while the last two dissociate to deposit two C atoms per TMG molecule onto the ZrB_2 surface. © *2013 American Vacuum Society*. [http://dx.doi.org/10.1116/1.4826881]

I. INTRODUCTION

Over the past few decades, III–V compound semiconductors have received remarkable interest due to their application in a wide variety of electronic and optoelectronic devices owing to their superior material properties.[1,2] In particular, GaN is used in blue light-emitting diodes (LEDs) for various applications such as indoor/outdoor illumination, displays, automobile headlights, and in high-power and high-frequency electronics.[1–3] For commercial devices, GaN is typically prepared as a thin film heteroepitaxially grown on sapphire, SiC, or Si. However, the mismatch of lattice constant and thermal expansion coefficient between these substrates and GaN is large, which results in strained films with a high density of threading dislocations.[4] These dislocations are carrier scatterers,[5] trap centers,[6,7] and leakage current sources[8,9] and therefore degrade device performance. In addition, structural strain may lead to the formation of cracks and to strong built-in electrostatic fields.[10,11] Therefore, a substrate material that closely matches the nitride's lattice constant and thermal expansion coefficient is highly desirable.[12] Recently, ZrB_2, a refractory compound with good lattice constant and thermal expansion matching with GaN, has been proposed as a viable substrate for epitaxial GaN growth.[12–14] Furthermore, ZrB_2 is reflective and metallic, and its use as a substrate in LEDs minimizes loss of light and simplifies the device geometry as ZrB_2 can be used as one of the ohmic contacts.[15] The crystal structure of bulk ZrB_2 is simple hexagonal with alternating layers of boron and zirconium as shown in Fig. 1. Therefore, the (0001) surface of ZrB_2 can be terminated with either a Zr or B layer. Previous studies have indicated that Zr termination is thermodynamically more stable than B termination,[16–18] also in agreement with the predictions for HfB_2.[19]

GaN has been grown successfully on the $ZrB_2(0001)$ surface using molecular beam epitaxy,[13] pulsed-laser deposition,[20] and metal organic chemical vapor deposition (MOCVD).[21] Trimethylgallium (TMG) is an important precursor for GaN MOCVD. Several previous studies have examined the reaction of TMG on silicon,[22–27] GaAs,[28,29] and other[30] surfaces. TMG adsorption on silicon[22–26] and platinum[30] leads to incorporation of one mole of carbon per mole of TMG, whereas TMG on GaAs leads to no carbon buildup.[28] More recently, plasma enhanced atomic layer deposition of GaN on Si surfaces using TMG and NH_3 was reported in which low temperature (185 °C) growth was achieved without significant carbon incorporation in the bulk of the GaN film.[31] The dissociation of TMG and ammonia above GaN and InN surfaces has been the subject of previous computational studies;[32,33] yet, the corresponding experimental identification of the surface reaction paths and intermediates is lacking. In our present work, step-by-step dissociation of TMG on the $ZrB_2(0001)$ surface is investigated with x-ray photoelectron spectroscopy (XPS) and reflection absorption infrared spectroscopy (RAIRS).

The experiments reported here involved heating the surface briefly to higher temperatures after initial TMG exposures at two different surface temperatures, 95 and 300 K. At 95 K, TMG adsorbs without dissociation so that RAIRS and XPS data characteristic of molecular TMG adsorbed on the surface can be obtained. Upon annealing to higher temperatures, changes in the molecularly adsorb TMG can be detected and the temperature at which dissociation begins can be determined. Exposures at a temperature, such as 300 K, above where dissociation occurs, involve a more dynamic situation with dissociation of TMG and desorption of dissociation products occurring at the same time, which

a)Electronic mail: mtrenary@uic.edu

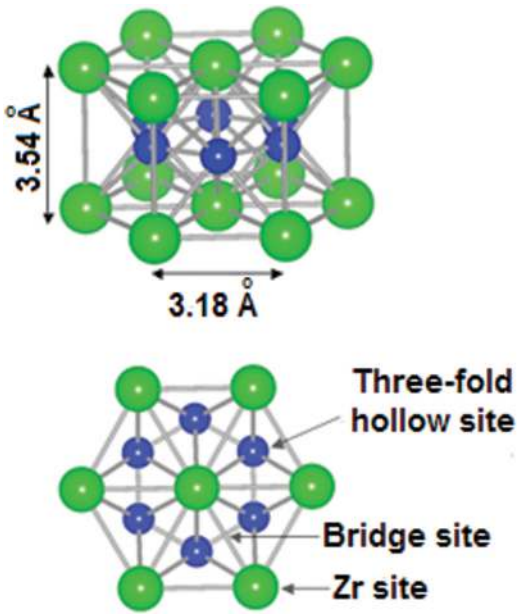

FIG. 1. (Color online) Side and top views of the $ZrB_2(0001)$ surface with Zr and B atoms represented by large and small spheres respectively. Reprinted with permission from Manandhar *et al.*, Surf. Sci. **615**, 110 (2013). Copyright, 2013 Elsevier.

can produce different species and different coverages than obtainable following a low temperature exposure. As it is thought that the initial stages of growth control the morphology of the resultant film, the results here provide important insights into the suitability of TMG for MOCVD growth of GaN films on ZrB_2 substrates.

II. EXPERIMENT

The experiments were performed in a stainless steel ultrahigh vacuum chamber with a base pressure of 1×10^{-10} Torr. The system has been described in detail elsewhere.[34] In brief, the chamber is equipped with a hemispherical electron energy analyzer (VG Microtech, Ltd., CLAM2) with a dual Mg/Al anode x-ray source (VG Microtech) for XPS studies, reverse view low energy electron diffraction (LEED) optics (Princeton Research Instruments, RV 8-120SH), and a commercial Fourier transform infrared spectrometer (Mattson, RS-10000).

The $ZrB_2(0001)$ single crystal was in the form of a square-shaped disk, approximately 1 cm on a side and about 2 mm thick. It was grown as described elsewhere[35] and was cut and polished to a mirror finish at the National Institute for Materials Science in Tsukuba, Japan, by methods similar to those described by Aizawa *et al.*[36] The crystal mounting and cleaning procedures have been described previously.[37,38] The clean $ZrB_2(0001)$ surface gave a sharp (1×1) LEED pattern and XPS spectra free of peaks due to any elements other than Zr and B and with binding energies (BEs) in good agreement with previous studies.[39–41] All XPS spectra were taken at a 15° angle between the analyzer and the surface normal using Mg Kα radiation and a constant analyzer pass energy of 50 eV corresponding to a nominal resolution of 1.32 eV. XPS core level peaks were fitted by using IGOR Pro (Wavemetrics, Inc.) software with the Shirley background removal method. The RAIR spectra were acquired with a resolution of 4 cm^{-1} and 1024 scans using a mercury cadmium telluride detector. In cases where the crystal was annealed above 95 K or room temperature (RT), it was cooled back down to 95 K or RT before acquiring the spectra. All background spectra were also acquired at either 95 K or room temperature. The epipure grade TMG was purchased from SAFC Hitech and used without further purification. Gas exposures are given in units of Langmuir (L), where $1\,L = 1 \times 10^{-6}$ Torr s. For the annealing experiments, the sample was heated to the desired temperature and held there for ~2 min.

III. RESULTS AND DISCUSSION

A. RAIR spectra

Figures 2(a), 2(b) and 3(a) show RAIR spectra obtained as a function of annealing temperature following 0.5 and 0.15 L TMG exposures at 95 and 300 K, respectively. The plots in Figs. 2(c) and 3(b) show the RAIRS peak areas from Figs. 2(a) and 3(a) as a function of annealing temperature. In Figs. 2(a) and 2(b), the peaks observed at ~1172, 1196, 2901, and 2960 cm^{-1} are assigned by comparison with the literature values in Table I.[23,30,42,43] The pair of bands with centers at 1172 and 1196 cm^{-1} correspond to CH_3 symmetric deformations (δ_s), 2901 cm^{-1} to a CH_3 symmetric stretch (ν_s), and 2960 cm^{-1} to a CH_3 asymmetric stretch (ν_{as}). The intensities of all peaks are unchanged from 95 to 190 K [Fig. 2(c)]. After annealing above 190 K, only one weak $\delta_s(CH_3)$ peak at 1196 cm^{-1} remains [Fig. 2(a)]. Annealing further up to 270 K did not change the intensity or position of this peak [Figs. 2(a) and 2(c)].

Figure 3(a) shows sharp and broad peaks centered at 999 and 1221 cm^{-1}, respectively. These peaks are assigned by comparison with the literature values. The sharp peak at 999 cm^{-1} agrees well with the Zr-H stretch vibration observed following exposure of $ZrB_2(0001)$ to $H_2(g)$.[36,37] In an IR study of TMG on a silicon dioxide surface, Mawhinney *et al.* reported a shift of ~11 cm^{-1} toward higher frequency for $\delta_s(CH_3)$ and $\delta_{as}(CH_3)$, which they attributed to the loss of one CH_3 group as TMG was transformed to dimethylgallium (DMG).[44] Furthermore, the intensities of the IR peaks of the CH_3 groups of DMG were much weaker than those of TMG. The broad feature at 1221 cm^{-1} is 25 cm^{-1} higher than the highest $\delta_s(CH_3)$ peak at 1196 cm^{-1} [Fig. 2(a)]. Although this might imply formation of DMG here, XPS results imply loss of two methyl groups to form monomethylgallium (MMG) and the ~1221 cm^{-1} peak is assigned to $\delta_s(CH_3)$ of this species. In the temperature range between ~555 and ~700 K, this band disappears [Figs. 3(a) and 3(b)], and a final shift in the Ga $2p_{3/2}$ XPS peak, along with a significant reduction in the intensity of the C 1s peak of CH_3 bonded to Ga [Figs. 6(a) and 6(b)], occurs. The Zr-H stretch peak intensity is fairly constant up to ~500 K [Fig. 3(c)]. Upon further annealing, the peak gradually decreases in intensity and then disappears at ~595 K [Figs. 3(a) and 3(b)], which is consistent with our

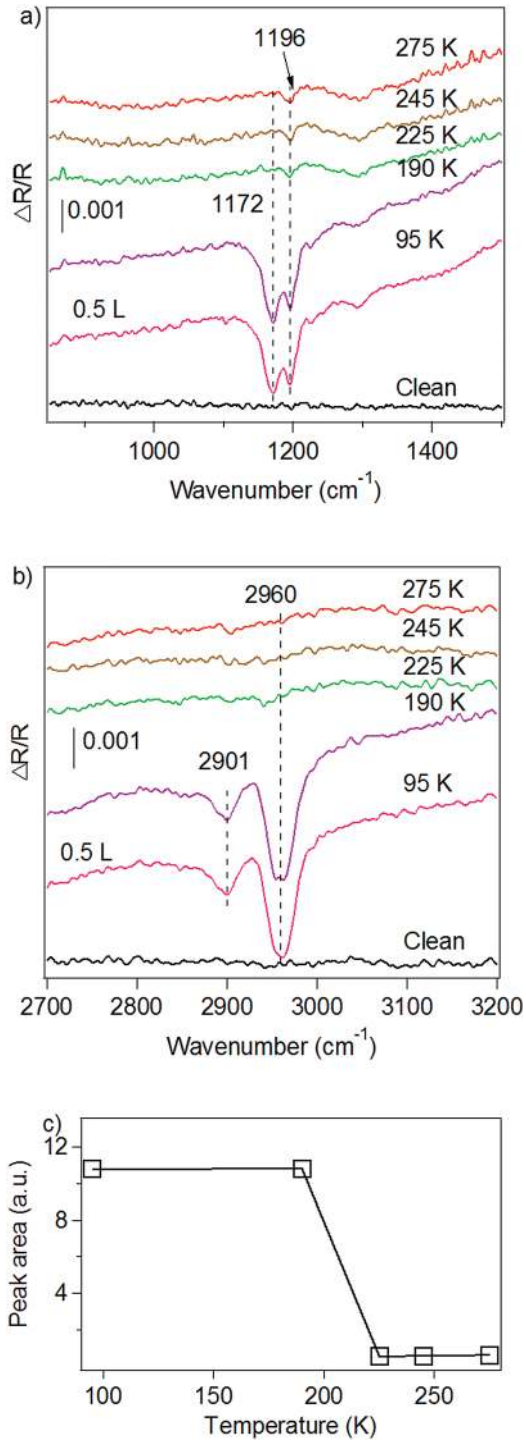

FIG. 2. (Color online) RAIR spectra of the CH_3 (a) deformation (δ_s and δ_{as}) and (b) stretch (ν_s and ν_{as}) regions as a function of annealing temperature following a 0.5 L TMG exposure at 95 K. (c) Plot of RAIRS peak intensity vs annealing temperature from (a).

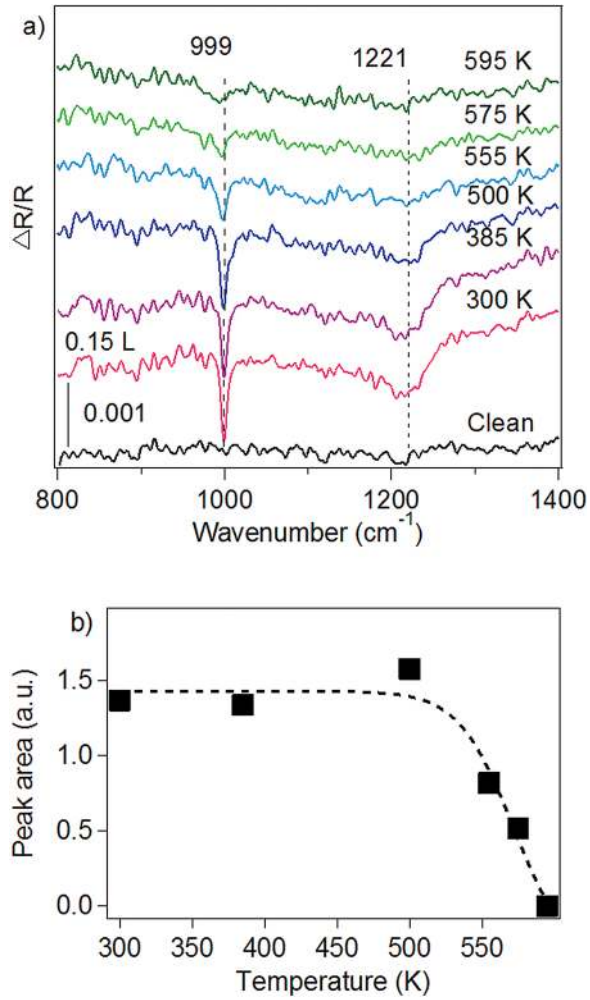

FIG. 3. (Color online) (a) RAIR spectra of the CH_3 deformation (δ_s and δ_{as}) and Zr-H stretch regions as a function of annealing temperature following a 0.15 L TMG exposure at 95 K. (b) Plot of Zr-H RAIRS peak intensity vs annealing temperature.

recent report of a hydrogen desorption temperature from $ZrB_2(0001)$ of ~625 K.[37] The approximately 30 K lower desorption temperature compared to the value in Ref. 37 is probably due to the coadsorption of carbon and gallium here. The observation of a Zr-H stretch following TMG exposure at 300 K in Fig. 3(a), but not after annealing to 280 K after exposure at 95 K in Fig. 2(a), along with observation of a peak at 1195 cm^{-1} in the latter case attributable to surface methyl groups, suggests that CH_3 dissociates at a temperature between 280 and 300 K to produce surface hydrogen and carbon.

B. XPS results for TMG exposures at 95 K followed by annealing to higher temperatures

Figure 4 shows C 1s (a), Ga $2p_{3/2}$ (b), B 1s/Zr 3d (c), XPS spectra and relative concentration (RC) plots for boron, zirconium, carbon, and gallium as a function of annealing temperature (d) for TMG exposed to the $ZrB_2(0001)$ surface at 95 K. In all C 1s spectra except in the one taken after the 280 K anneal, a shoulder at ~2 eV toward high binding energy (HBE) accompanies the main peak [Fig. 4(a)]. The origin for this shoulder is unknown.

To evaluate the thickness of the overlayers and to estimate ranges of the desorption temperature for molecular TMG only and for TMG fragments, the RCs of overlayer and substrate elements are calculated after each anneal to the temperatures used in Figs. 4(a)–4(c) and are plotted in Fig. 4(d). The concentration of an element is calculated from integrated peak areas weighted over the photoelectron

TABLE I. Vibrational modes (cm^{-1}) of TMG observed here and in the literature.

Mode	TMG/ZrB_2 (this work)	TMG/Si(100) HREELS[a]	TMG/Pt(111) HREELS[b]	Solid (IR)[c]	Liquid (Raman)[d]	Gas (IR)[e]
ν_s (CH_3)	2901	2950	2940	2898(E′)	2903(A_1')	2914(E′)
ν_{as} (CH_3)	2960	2950	2940	2955 (E′)	2961(E″)	2999(E′)
δ_s (CH_3)	1172, 1196	1240	1180	1168(E′)	1198(A_1')	1198(E′)

[a]Reference 23.
[b]Reference 30.
[c]Reference 42.
[d]Reference 43.
[e]Reference 43.

escape depth and by its XPS sensitivity factor.[45] The RC percentage of an element is calculated assuming the sum of the RCs of all detected elements is 100%. To obtain the RCs, we used both the $3d_{5/2}$ and $3d_{3/2}$ components of the Zr 3d peak but only the $2p_{3/2}$ component of the Ga 2p peak. The RCs of boron, zirconium, gallium, and carbon for clean ZrB_2 are, respectively, 58%, 42%, 0%, and 0%, which upon exposing to 0.5 L of TMG are ~0%, 3%, 25%, and 72%, respectively [Fig. 4(d)]. Although the stoichiometry implies that the RCs of B and Zr for the clean surface should be 67% and 33%, respectively, because the top layer is Zr, with the first boron layer below the surface, the Zr:B ratio from the RCs is slightly higher than would be obtained for a homogeneous distribution of the two elements over the escape depth of the

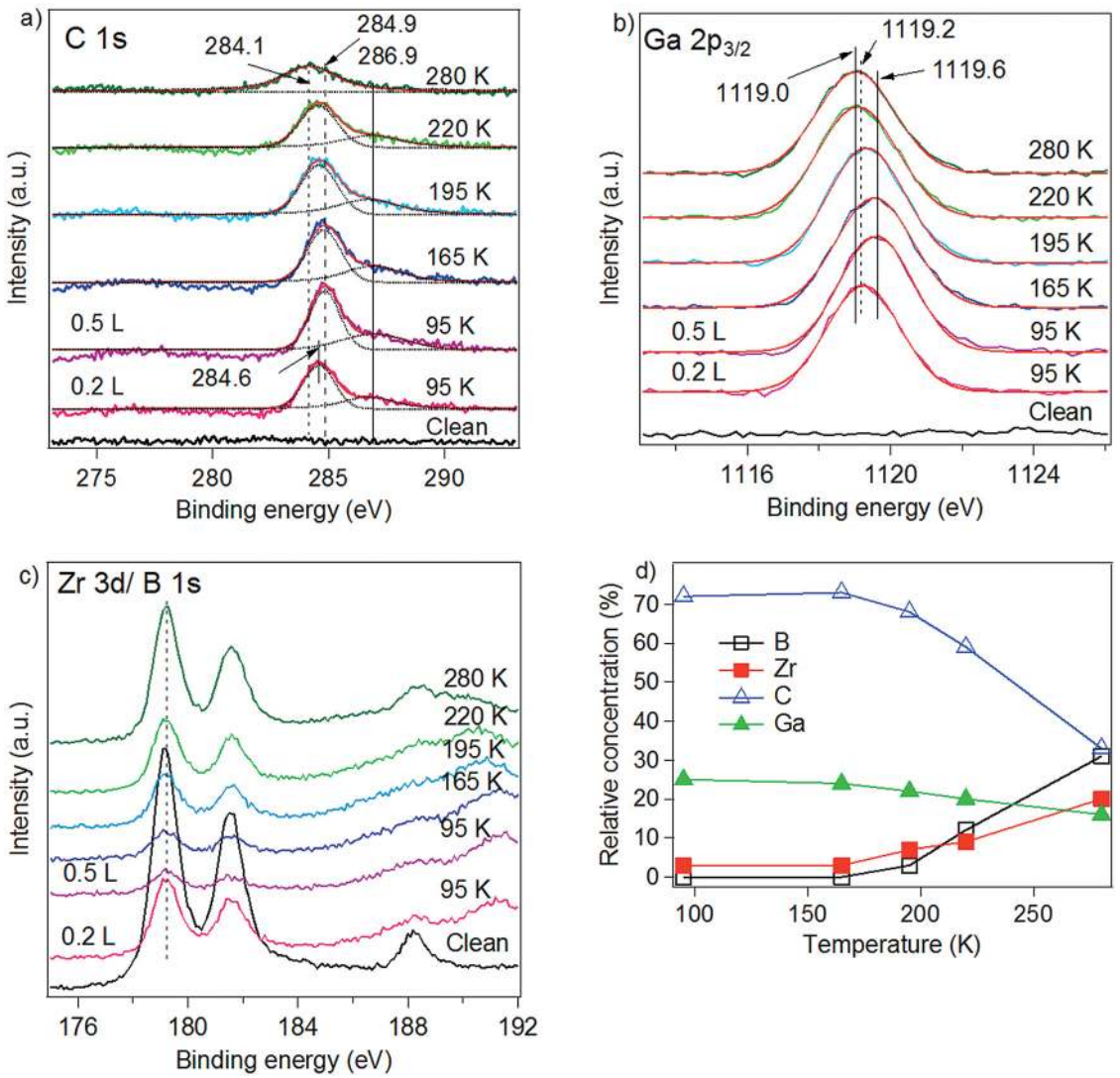

FIG. 4. (Color online) XPS spectra of the (a) C 1s, (b) Ga $2p_{3/2}$ (c) Zr 3d/B 1s regions as a function of annealing temperature following exposure to 0.5 L of TMG in two steps on $ZrB_2(0001)$ at 95 K. The black dashed and red solid curves in (a) are the fitted components and their sum, respectively. (d) Plots of relative concentration of boron (black line with open squares), zirconium (red line with filled squares), gallium (green line with filled triangles), and carbon (blue line with open triangles) as a function of annealing temperature.

photoelectrons. From 95 to 165 K, there is no change in the RCs of boron, zirconium, gallium, or carbon. After annealing in steps to 220 K, the boron and zirconium RCs slightly increase while the carbon and gallium RCs slightly decrease. The carbon and gallium RCs are respectively, ~59% and ~20%. The ratio of carbon to gallium on the ZrB_2 surface is still ~3, suggesting molecular desorption of TMG. After annealing to 280 K, as before, the RCs of zirconium and boron increase and that of carbon and gallium decrease. The RCs of both carbon and gallium are, respectively, ~33% and 16%. The ratio of carbon to gallium is now ~2 implying a loss of a methyl group from TMG and carbon desorption, presumably in the form of methane from the reaction of methyl with residual hydrogen on the surface or in the form of ethane from the combination of two methyl groups. The RCs of boron and zirconium after the 280 K anneal are ~31% and 20%, respectively [Fig. 4(d)]. These values are smaller by a factor of 1.8 ± 0.4 compared to the measured RCs of boron and zirconium when TMG was exposed at 300 K [Fig. 5(d)]. These RCs imply, for similar TMG exposures, that the overlayer thickness obtained by exposing at 300 K is less than the residual thickness after annealing to 280 K following exposure at 95 K. Molecular desorption of TMG from 165 to 220 K and breaking of a Ga-CH_3 bond after annealing above 220 K is supported by the RAIR spectra [Figs. 2(a) and 2(b)]. After annealing to ~225 K, the $\nu_s(CH_3)$ and $\nu_{as}(CH_3)$ peaks at 2901 and 2960 cm^{-1}, respectively, disappear and the intensities of the $\delta_s(CH_3)$ peaks at 1172 and 1196 cm^{-1} decrease considerably leaving only a weak peak at 1196 cm^{-1}.

In Fig. 4(a), the C 1s peak shifts to HBE with exposure and to lower binding energy (LBE) with annealing temperature. For overlayers formed from a 0.2 L exposure, the BE of the main C 1s peak is at 284.6 eV [Fig. 4(a)]. The BE of this peak shifts +0.3 eV for a 0.5 L exposure. Upon annealing in steps, the BE of the main peak gradually shifts back toward lower binding energies and is at 284.1 eV after heating to 280 K. As the overlayer thickness gradually decreases upon annealing above 95 K, a higher/lower C 1s BE is evidently related to a thicker/thinner overlayer. This is similar to an

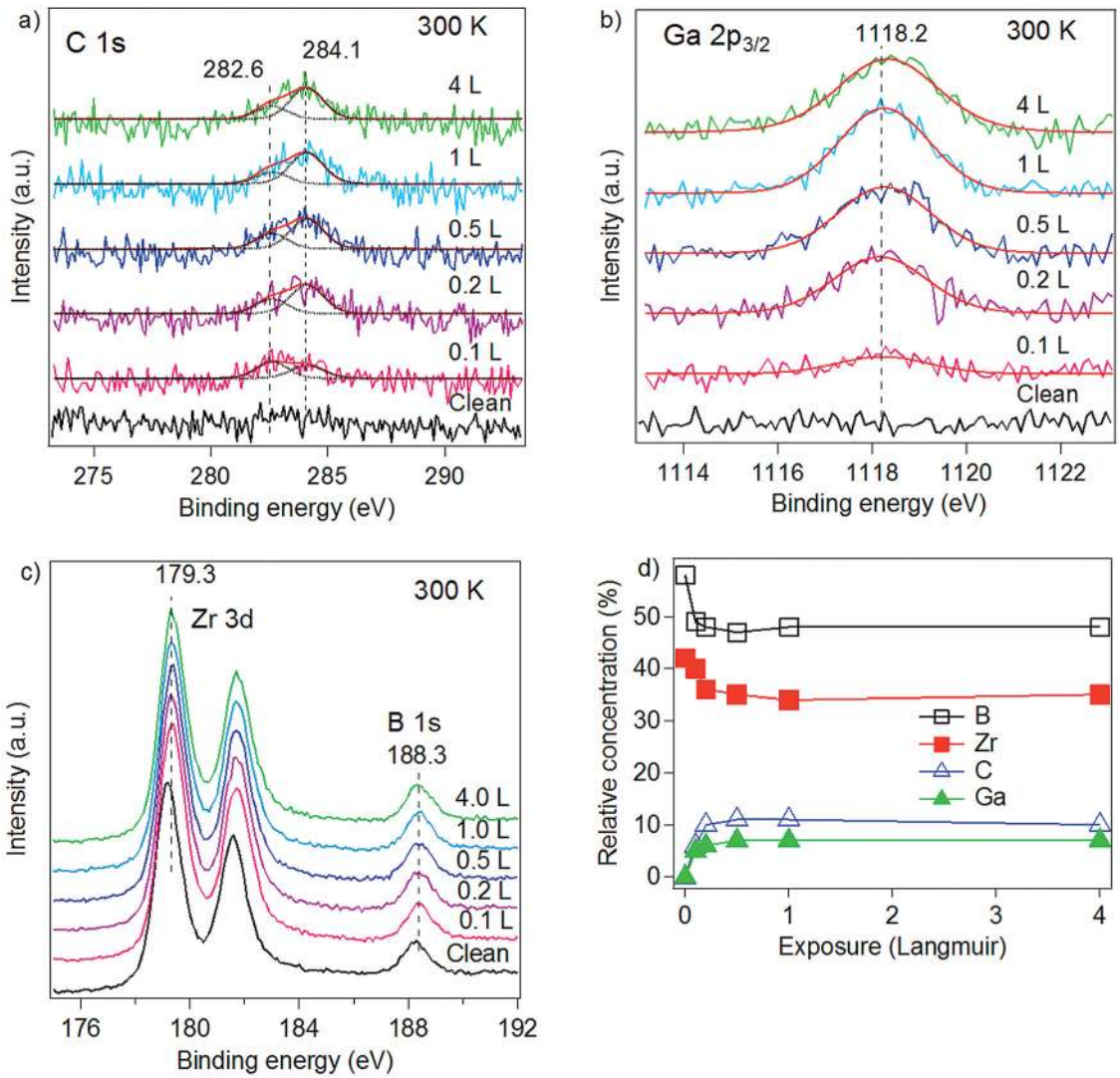

FIG. 5. (Color online) XPS spectra in the (a) C 1s, (b) Ga $2p_{3/2}$ (c) B 1s/Zr 3d regions as a function of TMG exposure at 300 K. The black dashed and red solid curves in (a) are the fitted components and their sum, respectively. (d) Plots of relative concentration of boron (black line with open squares), zirconium (red line with filled squares), gallium (green line with filled triangles), and carbon (blue line with open triangles) as a function of TMG exposure.

observation of the relative shift of the C 1s BE toward HBE/LBE values when the thickness of a methane multilayer increases/decreases on Pt(111).[46] A BE shift dependence on overlayer thickness is also observed for the Ga $2p_{3/2}$ peak. For a 0.2 L TMG exposure, the Ga $2p_{3/2}$ BE is at 1119.2 eV. Upon increasing the exposure to 0.5 L, the Ga $2p_{3/2}$ peak shifts by ~+0.4 to 1119.6 eV, which after annealing gradually shifts toward LBE and reaches 1119.0 eV after a 280 K anneal. It is noteworthy that Lee *et al.*[23] and Shogen *et al.*[47] in their XPS studies of TMG decomposition on Si(100) and Si(111), respectively, reported that the Ga core levels are ~0.2 eV lower for DMG than for TMG. In Fig. 4(b), the shift in the Ga $2p_{3/2}$ peak is gradual, so it is not straightforward to establish a temperature range for TMG decomposition and hence to determine a shift related to TMG partial dissociation. Since partial dissociation of TMG occurs between 220 and 280 K, we believe a shift of the Ga $2p_{3/2}$ peak of ~0.2 eV toward LBE in Fig. 4(b) is related to the partial dissociation of TMG. In the higher temperature (>280 K) experiments (explained below), there are two more significant shifts observed in the Ga $2p_{3/2}$ peak toward LBE. These shifts are indicative of further loss of CH_3 from Ga, so we suggest that a Ga $2p_{3/2}$ BE of ~1119 eV is associated with DMG on the $ZrB_2(0001)$ surface.

The C 1s peak obtained after annealing TMG exposed at 95 to 280 K is symmetric with the peak centered at 284.1 eV [Fig. 4(b)]. A 284.1 eV component also exists in the C 1s spectra taken after exposing TMG at 300 K [Fig. 5(a)]. We attribute the peak centered at 284.1 eV to C 1s of a CH_3 group still bonded to Ga.

C. XPS results for TMG exposures at 300 K

Figure 5 shows XPS spectra and a plot of RCs as a function of TMG exposure at 300 K. The RCs of zirconium and boron initially decrease while those of gallium and carbon increase. After an exposure of ~0.5 L of TMG, the RCs of zirconium, boron, gallium, and carbon are, respectively, 34%, 47%, 6%, and 13%. For longer exposure, almost no change in any of the RCs occurs indicating saturation of the ZrB_2 surface and in particular that a TMG multilayer does not form. At saturation, the decrease in the RCs of zirconium and boron relative to their values for the clean surface is ~10 ± 3%. Therefore, unlike nitrogen, which adsorbs at a three-fold hollow site resulting in a large decrease in the boron RC but a very small change in the zirconium RC when ammonia was exposed to ZrB_2 at RT,[38] the adsorbates here, which consist of the products of TMG dissociation, evidently do not prefer the three-fold hollow sites. The C 1s peaks are asymmetric with the main peak (HBE component) and shoulder (LBE component) centered at 284.1 and 282.6 eV, respectively. The intensity of the shoulder is almost constant for all exposures while that of the main peak gradually increases at the beginning and then levels off at an exposure of 0.5 L.

As for the TMG exposures at 95 K, for all exposures at 300 K, the Zr $3d_{5/2}$, Zr $3d_{3/2}$, and B 1s peaks are symmetric. However, after the first exposure of 0.1 L, the centers of the zirconium and boron peaks are shifted by ~0.1 eV toward higher BE compared to their values for the clean surface [Fig. 5(c)]. The peak positions do not change with increasing exposure. Similarly, the Ga $2p_{3/2}$ peak is symmetric for all exposures. The peak is centered at ~1118.2 eV, which is 0.8 eV lower than the measured value of 1119.0 eV of Ga $2p_{3/2}$ at 280 K. A significant shift in Ga BEs toward lower values as gallium becomes more metallic (fewer CH_3) was reported in the decomposition of TMG on Si(100) and Si(111).[22,47] Therefore, observation of a shift in Ga $2p_{3/2}$ by −0.8 eV in the 300 K spectra compared to those taken at 280 K suggests that gallium is more metallic when TMG is exposed to the ZrB_2 surface at 300 K than when the system of TMG/ZrB_2 prepared at 95 K is annealed to 280 K. As there is a final shift in the Ga $2p_{3/2}$ BE further toward lower values when the TMG/ZrB_2 system prepared at 300 K is annealed to higher temperatures, we assign the 1118.2 eV BE peak to Ga $2p_{3/2}$ of MMG.

The LBE component of C 1s at 282.6 eV observed here is close to the BE of carbon bonded to a Si(100) surface, 282.5 eV.[22] Therefore, we attribute the 282.6 eV component to carbon bonded to the ZrB_2 surface. This assumption is further supported by the fact that the only remaining C 1s peak after annealing above 1025 K is at 282.6 eV [Fig. 6(a)]. After annealing above 1025 K, gallium desorbs from the surface, implying that the remaining carbon is bonded directly to the ZrB_2 surface. The BE of the C 1s main peak at 284.1 eV is ~1.5 eV higher than the BE of the shoulder at 282.6 eV. The BE of the symmetric C 1s peak in the spectrum taken after annealing to 280 K in Fig. 4(a) is also 284.1 eV. Based on the explanation above, TMG has partially decomposed to form MMG. A constant C 1s BE for one to three methyl groups bonded to gallium has been reported in studies of the dissociation of TMG on silicon surfaces.[22,23,47] We therefore attribute the C 1s peak centered at 284.1 eV in Fig. 5(a) to a CH_3 group still bonded to Ga. This assignment is supported by observation with RAIRS of the $\delta_s(CH_3)$ peak corresponding to MMG at ~1221 cm^{-1} from TMG exposure at 300 K.

D. XPS results for TMG exposure at 300 K and annealing to higher temperatures

Figure 6 shows XPS results following annealing to the indicated temperatures after a 1.5 L TMG exposure to the $ZrB_2(0001)$ surface at 300 K. As in Fig. 5(a), the C 1s spectrum has two components at 282.6 and 284.2 eV. The C 1s component of the Ga-bound carbon decreases significantly after annealing at 565 K. The apparent reappearance of this peak in the 1025 K spectrum [Fig. 6(a)] is probably due to noise. For all the spectra, within experimental error, the total C 1s intensity is constant [Fig. 6(d)]. This implies that the CH_3 that splits off from the gallium binds to the ZrB_2 surface and spontaneously dissociates to C and H atoms.

Following the 300 K exposure but before annealing, the Ga $2p_{3/2}$ BE is 1118.3 eV, which agrees with the value in Fig. 5(b), within experimental error. There is no BE shift up to 435 K. A significant decrease of the Ga $2p_{3/2}$ BE is observed after the sample is annealed to 565 K and this decrease continues for annealing up to 725 K. At 725 K, the

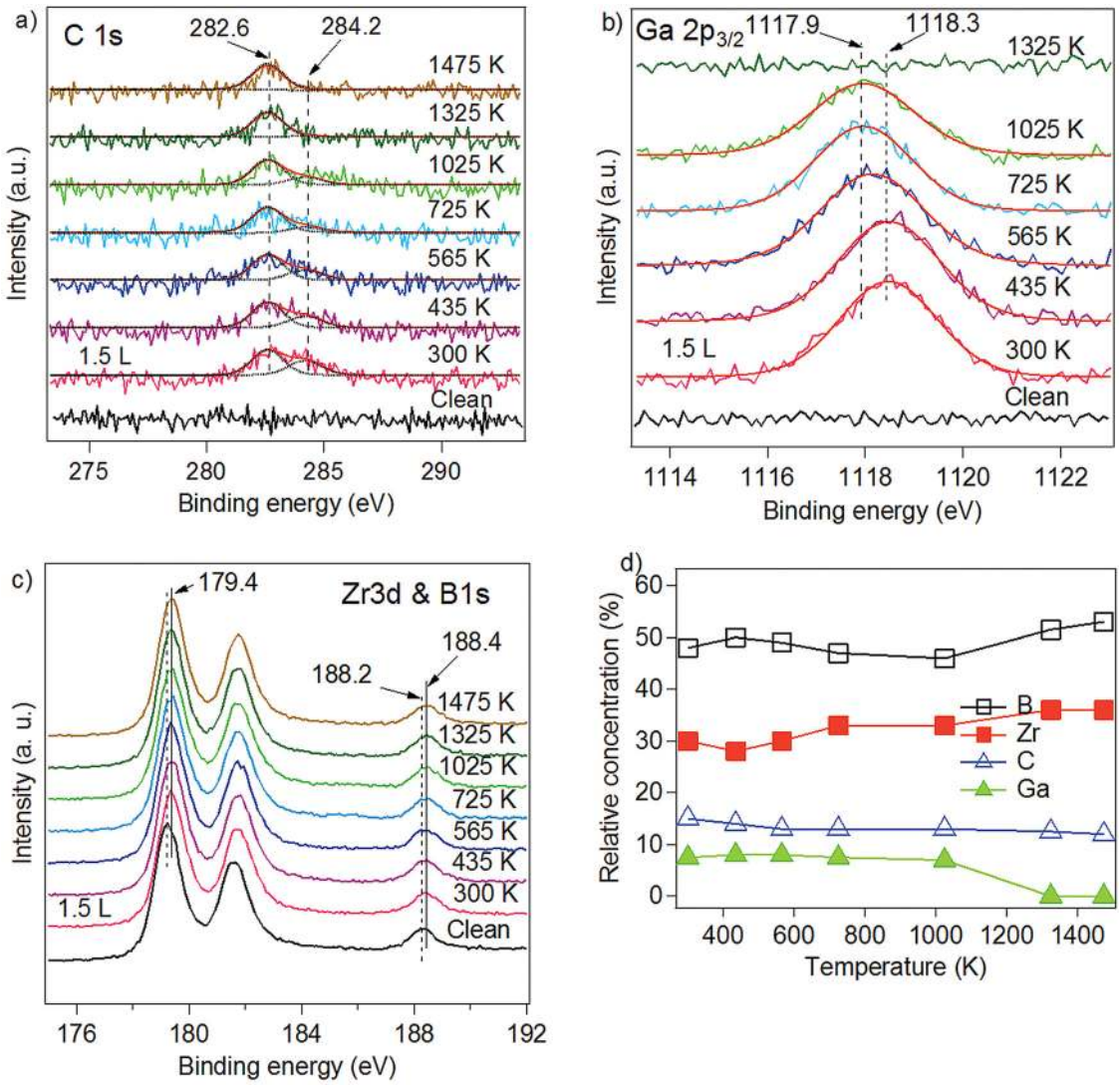

FIG. 6. (Color online) XPS spectra in the (a) C 1s, (b) Ga $2p_{3/2}$, (c) B 1s/Zr 3d regions as a function of annealing temperature following exposure of 1.5 L of TMG on $ZrB_2(0001)$ at 300 K. The black dashed and red solid curves in (a) are the fitted components and their sum, respectively. (d) Plots of relative concentration of boron (black line with open squares), zirconium (red line with filled squares), gallium (green line with filled triangles), and carbon (blue line with open triangles) as a function of annealing temperature.

Ga $2p_{3/2}$ BE is 1117.9 eV. This observation suggests that at ~565 K breaking of the last gallium-methyl bonds begins. This assumption is supported by the disappearance of the broad $\delta_s(CH_3)$ RAIRS peak centered at ~1221 cm^{-1} after annealing to 555 K [Fig. 3(a)] and also by the disappearance of the 284.2 eV component of the C 1s peak in Fig. 6(a). A high dissociation temperature of ~565 K for the last Ga–CH_3 bond agrees quite well with a similar high temperature (above 495 K) reported in studies of TMG on various surfaces.[23,25,30] As for TMG exposure at 300 K, the Zr 3d and B 1s peaks are shifted ~0.2 eV toward HBE after exposing TMG, and there is no further shift upon annealing to the temperatures indicated in Fig. 6(c). Thus, the initial shift in the Zr 3d and B 1s peaks upon exposure at 300 K is attributed to the bonding of atomic carbon to the ZrB_2 surface from either the partial or complete dissociation of TMG.

The XPS results should, in principle, be sensitive to the form of the carbon deposited onto the surface following either exposure at room temperature or after annealing to high temperature. In Fig. 6(a), a single C 1s peak at 282.6 eV remains after annealing the surface to 1475 K after TMG deposition at 300 K. This value is consistent with formation of ZrC, as the C 1s BEs for metal carbides generally fall in this range.[48] It is not consistent with formation of graphitic carbon, which has a C 1s BE of 284.5 eV.[48] The C 1s peak in boron carbide shows two components at 281.8 and 283.7 eV, with the former having twice the intensity of the latter.[49] Within the limited signal-to-noise ratio in Fig. 6 for the C 1s peak, the results seem more consistent with the formation of zirconium carbide than boron carbide. Because the amount of carbon is so small, little change in the Zr 3d or B 1s peaks is seen. Also, the expected chemical shifts for these peaks upon the formation of even a large amount of carbide of either B or Zr would likely be too small to detect. If the formation of ZrC produced elemental boron at the surface, a B 1s peak at less than 188 eV would be expected but is not seen.[50]

The XPS results therefore imply that residual carbon bonds to Zr in a way that does not substantially alter the bonding within the ZrB_2 substrate.

From the above results, it is unambiguous that decomposition of TMG on the ZrB_2 surface results in carbon incorporation. Furthermore, carbon on the $ZrB_2(0001)$ surface neither desorbed nor diffused into the bulk even after annealing to ~1500 K, which is well above the temperature used for MOCVD growth of GaN. It is therefore possible that the deposited carbon may affect the morphology and defect density in films grown on ZrB_2 surfaces from TMG. Previous studies demonstrated that the primary source of carbon impurities in MOCVD grown III–V semiconductors is the metal alkyl precursors.[51,52] Several studies reported dramatic reductions in carbon incorporation in compounds such as GaAs and GaN when triethylgallium (TEG) is used as the gallium source instead of TMG.[53–55] Similarly, using TEG could lead to reduced carbon deposition on ZrB_2 substrates used for GaN growth.

IV. SUMMARY AND CONCLUSION

We used XPS and RAIRS to investigate the dissociation of TMG on the $ZrB_2(0001)$ surface. Consistent with results in other systems in which the gallium core levels shift toward LBE as gallium becomes more metallic, similar shifts in the Ga $2p_{3/2}$ peak are observed here. In addition to Ga $2p_{3/2}$ XPS BE shifts, C 1s XPS and RAIR spectra confirmed a stepwise dissociation of the gallium-methyl bonds. TMG is adsorbed molecularly at 95 K and it does not dissociate up to 220 K. Upon annealing above 220 K, TMG becomes more metallic via breaking of gallium-methyl bonds and eventually becomes completely metallic after all three Ga-C bonds are broken. At temperatures between 220 and 280 K, loss of a methyl group from TMG produces DMG. The symmetric C 1s peak obtained after annealing to 280 K suggests desorption of methyl. Between 280 and 565 K, DMG further dissociates to MMG. Upon exposure of TMG to the surface at 300 K, a Zr–H stretch at 999 cm^{-1} is observed with RAIRS and an asymmetric C 1s peak with a component corresponding to carbon bonded to the ZrB_2 surface (282.6 eV) is observed with XPS. These observations indicate that at 300 K, Ga-CH_3 bonds are broken and that the resulting surface methyl groups immediately dissociate to produce C and H atoms on the surface. Between 565 and 725 K, the last Ga-CH_3 bond is broken. In this temperature range, the Ga/carbon concentration ratio is essentially constant implying that the last methyl also produces C atoms bound to the ZrB_2 surface. Hydrogen desorbs from the surface at around 595 K and gallium desorbs between 1025 K and 1323 K while carbon remains to at least 1475 K. The incorporated carbon is removed only by sputtering. Dissociation of TMG on the ZrB_2 surface results in two moles of carbon incorporation per one mole of TMG, making carbon incorporation an intrinsic part of the surface chemistry.

ACKNOWLEDGMENTS

This work was supported by the U.S. Department of Energy, Office of Science, Office of Basic Energy Sciences-Materials Science under Contract No. DE-AC02-06CH11357. K.M. and M.T. also acknowledge partial support from the National Science Foundation under grant CHE-1012201.

[1]O. Ambacher, J. Phys. D: Appl. Phys. **31**, 2653 (1998).
[2]H. Morkoc, *Handbook of Nitride Semiconductors and Devices* (Wiley-VCH Verlag, Weinheim, Germany, 2009).
[3]S. Nakamura, S. Pearton, and G. Fasol, *The Blue Laser Diode: The Complete Story* (Springer-Verlag, Berlin, 2000).
[4]S. C. Jain, M. Willander, J. Narayan, and R. V. Overstraeten, J. Appl. Phys. **87**, 965 (2000).
[5]N. G. Weimann, L. F. Eastman, D. Doppalapudi, H. M. Ng, and T. D. Moustakas, J. Appl. Phys. **83**, 3656 (1998).
[6]S. M. Lee, M. A. Belkhir, X. Y. Zhu, Y. H. Lee, Y. G. Hwang, and T. Frauenheim, Phys. Rev. B **61**, 16033 (2000).
[7]S. J. Rosner, E. C. Carr, M. J. Ludowise, G. Girolami, and H. I. Erikson, Appl. Phys. Lett. **70**, 420 (1997).
[8]P. Kozodoy, J. P. Ibbetson, H. Marchand, P. T. Fini, S. Keller, J. S. Speck, S. P. DenBaars, and U. K. Mishra, Appl. Phys. Lett. **73**, 975 (1998).
[9]B. S. Simpkins, E. T. Yu, P. Waltereit, and J. S. Speck, J. Appl. Phys. **94**, 1448 (2003).
[10]S. Ghosh, P. Waltereit, O. Brandt, H. T. Grahn, and K. H. Ploog, Phys. Rev. B **65**, 075202 (2002).
[11]J. Seo Im, H. Kollmer, J. Off, A. Sohmer, F. Scholz, and A. Hangleiter, Phys. Rev. B **57**, R9435 (1998).
[12]R. Liu, A. Bell, F. A. Ponce, S. Kamiyama, H. Amano, and I. Akasaki, Appl. Phys. Lett. **81**, 3182 (2002).
[13]J. Suda and H. Matsunami, J. Cryst. Growth **237**, 1114 (2002).
[14]H. Kinoshita, S. Otani, S. Kamiyama, H. Amano, I. Akasaki, J. Suda, and H. Matsunami, Jpn. J. Appl. Phys. **40**, L1280 (2001).
[15]A. H. Blake *et al.*, J. Appl. Phys. **111**, 033107 (2012).
[16]X. Zhang, X. Luo, J. Li, J. Han, W. Han, and C. Hong, Comp. Mater. Sci. **46**, 1 (2009).
[17]T. Aizawa, W. Hayami, and S. Otani, Phys. Rev. B **65**, 024303 (2001).
[18]P. L. Liu, A. V. G. Chizmeshya, J. Kouvetakis, and I. S. T. Tsong, Phys. Rev. B **72**, 245335 (2005).
[19]K. Yamamoto, K. Kobayashi, H. Kawanowa, and R. Souda, Phys. Rev. B **60**, 15617 (1999).
[20]Y. Kawaguchi, J. Ohta, A. Kobayashi, and H. Fujioka, Appl. Phys. Lett. **87**, 221907 (2005).
[21]Y. Tomida *et al.*, Appl. Surf. Sci. **216**, 502 (2003).
[22]F. Lee, T. R. Gow, and R. I. Masel, J. Electrochem. Soc. **136**, 2640 (1989).
[23]F. Lee, A. L. Backman, R. Lin, T. R. Gow, and R. I. Masel, Surf. Sci. **216**, 173 (1989).
[24]C. R. Flores, X. L. Zhou, and J. M. White, Surf. Sci. **261**, 99 (1992).
[25]A. Forster and H. Luth, J. Vac. Sci. Technol. B **7**, 720 (1989).
[26]K. Fukui, W. Mizutani, H. Onishi, S. Ichimura, H. Shimizu, and Y. Iwasawa, Jpn. J. Appl. Phys. **34**, 4910 (1995).
[27]L. A. Cadwell and R. I. Masel, Surf. Sci. **318**, 321 (1994).
[28]X. Y. Zhu, J. M. White, and J. R. Creighton, J. Vac. Sci. Technol. A **10**, 316 (1992).
[29]J. R. Creighton, Surf. Sci. **234**, 287 (1990).
[30]Z. M. Liu, X. L. Zhou, and J. M. White, Appl. Surf. Sci. **52**, 249 (1991).
[31]C. Ozgit, I. Donmez, M. Alevli, and N. Biyikli, J. Vac. Sci. Technol. A **30**, 01A124 (2012).
[32]B. H. Cardelino and C. A. Cardelino, J. Phys. Chem. C **113**, 21765 (2009).
[33]B. H. Cardelino and C. A. Cardelino, J. Phys. Chem. C **115**, 9090 (2011).
[34]D. H. Kang and M. Trenary, Surf. Sci. **470**, L13 (2000).
[35]S. Otani, M. M. Korsukova, and T. Mitsuhashi, J. Cryst. Growth **186**, 582 (1998).
[36]T. Aizawa, W. Hayami, and S. Otani, J. Chem. Phys. **117**, 11310 (2002).
[37]W. Walkosz, K. Manandhar, M. Trenary, S. Otani, and P. Zapol, Surf. Sci. **606**, 1808 (2012).
[38]K. Manandhar, W. Walkosz, M. Trenary, S. Otani, and P. Zapol, Surf. Sci. **615**, 110 (2013).
[39]R. Singh, M. Trenary, and Y. Paderno, Surf. Sci. Spectra **7**, 310 (2000).
[40]Y. Kawaguchi, A. Kobayashi, J. Ohta, and H. Fujioka, Jpn. J. Appl. Phys. **45**, 6893 (2006).
[41]Z. T. Wang, Y. Yamada-Takamura, Y. Fujikawa, T. Sakurai, Q. K. Xue, J. Tolle, J. Kouvetakis, and I. S. T. Tsong, J. Appl. Phys. **100**, 033506 (2006).

[42]S. Kvisle and E. Rytter, Spectrochim. Acta A **40**, 939 (1984).
[43]G. E. Coates and A. J. Downs, J. Chem. Soc. 3353 (1964).
[44]D. B. Mawhinney, J. A. Glass, Jr., and J. T. Yates, Jr., J. Vac. Sci. Technol. A **17**, 679 (1999).
[45]M. P. S. D. Briggs, *Practical Surface Analysis by Auger, and X-ray Photoelectron Spectroscopy* (John Wiley & Sons, New York, 1983).
[46]R. Larciprete, A. Goldoni, A. Groŝo, S. Lizzit, and G. Paolucci, Surf. Sci. **482–485**, 134 (2001).
[47]S. Shogen, Y. Matsumi, M. Kawasaki, I. Toyoshima, and H. Okabe, J. Appl. Phys. **70**, 462 (1991).
[48]J. F. Moulder, W. F. Stickle, P. E. Sobol, and K. D. Bomben, *Handbook of X-ray Photoelectron Spectroscopy* (Perkin-Elmer Corporation, Minnesota, 1992).
[49]I. Jiménez, D. G. J. Sutherland, T. van Buuren, J. A. Carlisle, L. J. Terminello, and F. J. Himpsel, Phys. Rev. B **57**, 13167 (1998).
[50]W. C. Foo, J. S. Ozcomert, and M. Trenary, Surf. Sci. **255**, 245 (1991).
[51]J. R. Creighton, B. A. Bansenauer, T. Huett, and J. M. White, J. Vac. Sci. Technol. A **11**, 876 (1993).
[52]C. R. Abernathy and W. S. Hobson, J. Mater. Sci.: Mater. Electron **7**, 1 (1996).
[53]N. Kobayashi and T. Makimoto, Jpn. J. Appl. Phys., Part 2. **24**, L824 (1985).
[54]N. Kobayashi and T. Fukui, Electron. Lett. **20**, 887 (1984).
[55]P. Norris, J. Black, S. Zemon, and G. Lambert, J. Cryst. Growth **68**, 437 (1984).